# INDIVIDUAL TREE-BASED FOREST SPECIES DIVERSITY ESTIMATION USING UAV-BORNE HYPERSPECTRAL AND LIDAR DATA

Z. Zheng [1], X. Li [1,2], C. Xu [1,2], P. Zhao [1,2], J. Chen [1,2], J. Wu [1,2], X. Zhao [1,2], X. Mu [1,2], D. Zhao [1,2], Y. Zeng [1,2]*

[1] State Key Laboratory of Remote Sensing Science, Aerospace Information Research Institute, Chinese Academy of Sciences, Beijing, China - (zhengzhaoju, xucong, zhaodan, zengyuan)@aircas.ac.cn
[2] University of Chinese Academy of Sciences, Beijing, China - (lixiuwen20, zhaoping22, chenjunhua21, wujinchen22, zhaoxueming21, muxuan22)@mails.ucas.ac.cn

**KEY WORDS:** Forest species diversity, Classification, Clustering, UAV, Individual tree-based.

**ABSTRACT:**

Forest biodiversity is essential in maintaining ecosystem functions and services. Recently, unmanned aerial vehicle (UAV) remote sensing technology has emerged as a cost-effective and flexible tool for biodiversity monitoring. In this study, we compared the optimal clustering algorithm, classification method (spectral angle mapper, SAM), spectral diversity metric and structural heterogeneity index for forest species diversity estimation in two complex subtropical forests, Mazongling (MZL) and Gonggashan (GGS) National Nature Forest Reserves in China, using UAV-borne hyperspectral and LiDAR data. The results showed that the SAM classification method performed better with higher values of $R^2$ than the clustering algorithm for predicting both species richness (MZL: 0.62 > 0.46 and GGS: 0.55 > 0.46) and Shannon-Wiener index (MZL: 0.64 > 0.58 and GGS: 0.52 > 0.47), while the optimal clustering algorithm had the highest prediction accuracy for the Simpson index, followed by the SAM classification method, spectral diversity metric and structural heterogeneity index (MZL: 0.83>0.44>0.31>0.12, GGS: 0.62>0.44>0.38>0.00). Our study indicated that the SAM classification method had the advantage of identifying rare species and estimating species richness, while the clustering method could capture forest diversity patterns rapidly without distinguishing the specific tree species and predict the Simpson index more accurately. Overall, both clustering and classification methods exhibited superior performance compared to spectral or structural diversity indices. Our findings highlight the applicability of UAV remote sensing in monitoring forest species diversity in complex subtropical forests.

## 1. INTRODUCTION

Biodiversity plays a crucial role in maintaining ecosystem functions and services. Forest ecosystems are one of the most important global repositories of terrestrial biodiversity, providing habitat for over half of terrestrial plant and animal species. However, the biodiversity of forests is facing serious decline globally due to climate change and human activities, and this trend is likely to continue in the future. Forest species diversity, which refers to the number and distribution of tree species within forest ecosystems, is a primary component of forest biodiversity. Traditional forest species diversity estimation relies on field surveys, which are time-consuming, labor-intensive, and spatio-temporal limited. Monitoring forest diversity is therefore essential for ecological conservation and management.

Remote sensing techniques have been increasingly used for monitoring and assessing forest species diversity loss across scales in a repeatable and rapid manner. The UAV (unmanned aerial vehicle) remote sensing technology can be equipped with hyperspectral sensors to obtain continuous spectral information of vegetation and LiDAR (Light Detection and Ranging) sensors to penetrate the vegetation canopy to obtain 3-dimensional structural features directly, showing great potential in forest species identification and diversity monitoring in recent years. Furthermore, advances in LiDAR remote sensing have enabled the accurate extraction of information from individual tree crowns (ITCs). Compared to the pixel-based approach, the ITC-based approach is more directly analogous to the field-based individual sampling method, which can better extract structural features of the canopy and minimize the signal confusion brought by non-tree pixels (Zheng et al., 2022).

Monitoring species diversity by remote sensing can be divided into roughly two categories: identifying the species directly and estimating the species diversity indices indirectly based on habitat or relevant indicators (Xu et al., 2022). Distinguishing individual tree species in complex subtropical or tropical forests is challenging due to spectral similarities among species and variations within the same species (Wang and Gamon, 2019). Moreover, classification confusion increases with greater biodiversity, necessitating more training data for species-rich forests to enhance accuracy. However, gathering adequate data for training and validation in these diverse, complex terrains is difficult.

Compared with direct species identification methods limited to big-size species or non-mixed species, spectral variation hypothesis (SVH), as the most representative indirect observation method, has strong applicability in monitoring species diversity. The spectral variation hypothesis assumes that the remotely sensed variation in spectral patterns is related to plant species diversity. Many SVH-based approaches such as spectral diversity metrics and clustering algorithms, have been applied for species diversity estimation at the individual canopy level of the forest, especially in combination with LiDAR data. Moreover, some studies indicated that tree height or the structural heterogeneity index is beneficial for predicting species richness in Mediterranean forests (Lopatin et al., 2016; Simonson et al., 2012). However, it remains unclear which

* Corresponding author

method is more effective for monitoring different aspects of species diversity in complex forest conditions.

Therefore, the major objectives of our study are to explore the performance of individual tree-based classification, clustering, spectral diversity metric and structural heterogeneity methods in estimating three commonly used forest species diversity indices (species richness, Shannon-Wiener index and Simpson index) in two typical subtropical forests in China using UAV-borne hyperspectral and LiDAR data. We aim to (1) classify tree species using the SAM classification method based on hyperspectral image and the individual tree crown segmentation results from LiDAR data, (2) estimate forest species diversity using different clustering algorithms, spectral diversity metrics and structural heterogeneity metrics based on optimal biochemical vegetation indices and structural features, and (3) further compare the performance and applicability of these methods for predicting different species diversity indices in these two subtropical forest sites.

## 2. MATERIALS AND METHODS

We conducted this study in two complex subtropical forest areas, Mazongling (MZL, 115°41′37′–115°42′5′E, 31°15′25′–31°15′44′N) and Gonggashan (GGS, 102°3′50′–102°4′28′E, 29°36′2′–29°36′15′N) National Nature Forest Reserves (Figure 1). MZL study area located in Jinzhai county, Anhui province of China covers about 23.8 ha and contains more than 10 dominant tree species, such as *Quercus glandulifera*, *Platycarya strobilacea*, *Castanea mollissima* and *Lindera glauca*. GGS study area located in Ganzi (Garzê) Tibetan autonomous prefecture, Sichuan province of China covers an area of approximately 20.5 ha and the forest canopy comprises more than 15 dominant tree species, such as *Fagus longipetiolata*, *Jasminum nudiflorum*, *Ailanthus altissima*, *Cercidiphyllum japonicum* and *Bothrocaryum controversum*.

Field measurements in 26 plots (30×30 m) were collected in September–October 2020 and July 2022. The differentially-corrected GPS was used to determine the coordinates of the four corners of each plot and tree parameters (incl. species name, tree height, DBH, crown base height, crown dominant classes and crown diameters) were measured for all individual trees with DBH≥ 5 cm. We additionally measured the exact location of each tree in two of the MZL plots and four of the GGS plots by integrating the Real-Time Kinematic (RTK) GPS/GLONASS System with a total station to validate the individual tree segmentation accuracy and provide samples for tree species classification. The top-of-canopy leaves for 10 dominant tree species in MZL and 15 dominant tree species in GGS were collected to measure their spectral properties and biochemical components, which include chlorophyll a and b (Chl-a, Chl-b), total carotenoids (Car), total carbon (C), nitrogen (N), phosphorus (P), cellulose (Cel), lignin (Lig), specific leaf area (SLA) and equivalent water thickness (EWT), following the method described in Zhao et al. (2016).

We employed three distinct diversity indices, namely species richness, Shannon-Wiener index, and Simpson index, to represent forest species diversity and calculated them within each sample plot based on the field measurements. Species richness refers to the total number of species in the sample plot. Shannon-Wiener index and Simpson index can reflect species richness and evenness of species distribution. The Shannon-Wiener index is more sensitive to the number of species, and the Simpson index is more sensitive to the evenness of enriched species (Nagendra, 2002). The calculation formula of the Shannon-Wiener index (H) and Simpson index (D) were as follows:

$$H = \sum_{i=1}^{n} -p_i \ln p_i, \quad (1)$$

$$D = 1 - \sum_{i=1}^{n} p_i^2, \quad (2)$$

where $n$ is the total number of species in the sample plot, and $p_i$ is the proportional abundance of the species $i$.

The UAV-borne hyperspectral data were collected on September 18 and October 15, 2020, using the Cuber UHD185 Firefly imaging spectrometer (Cubert GmbH, Ulm, Baden-Württemberg, Germany) onboard a DJI Matrice 300 aircraft under cloudless conditions. The sensor comprises 125 visible and near-infrared spectral channels ranging from 450 nm to 946 nm with an 8 nm spectral resolution. The UAV flew at an altitude of 80 m, resulting in a 7 cm spatial resolution. The image preprocessing consisted of image mosaic, spectral radiation calibration, reflectance calibration and geometric correction. The UAV-borne LiDAR data were obtained simultaneously with the hyperspectral dataset acquisition using the LiAir VH Pro scanner (Green Valley Inc., Beijing, China) operating at a wavelength of 905 nm. The average point density in MZL is more than 117 points/m$^2$, and the average point density in MZL is more than 168 points/m$^2$. The UAV-borne LiDAR data were terrain normalized based on the ground points and the vegetation point clouds with a normalized height below 2 m were removed to reduce the effect of background factors such as shrubs and grasses in the point clouds. The pre-processing of the UAV-borne hyperspectral and LiDAR data was described in detail in Li et al. (2023).

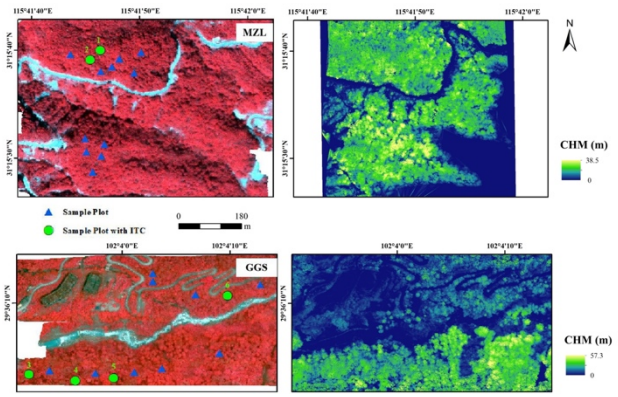


**Figure 1**. Manzongling study area (MZL, top) and Gonggashan study area (GGS, bottom) with imaging spectroscopy data acquired from Cuber UHD185 Firefly imaging spectrometer (left, Red: 866 nm, Green: 654 nm, Blue: 566 nm) and canopy height model (CHM) derived from LiDAR point clouds obtained from LiAir VH Pro scanner. The blue triangles indicate the locations of field-measured sample plots. The green circles indicate the locations of individual tree crown (ITC) validation plots.

The species diversity was estimated from the perspective of spectral and structural variation of individual trees by combining the UAV-borne hyperspectral and LiDAR data and ground survey data. We calculated the average spectrum of each canopy based on the ITC segmentation results in the sample plots. To obtain accurate canopy spectral data of dominant species, pixels with NDVI<0.2 and canopy height<2 m were removed from the hyperspectral images to reduce the effect of background factors such as canopy gaps. Moreover, the two

detailed ITC plots with 14 tree species in MZL (covering more than 90% of local tree species) and four detailed ITC plots with 22 tree species in GGS (covering more than 75% of local tree species) that measured the exact location of each tree were used to establish the endmember spectral library by calculating the average spectrum of each species in the two study areas (Figure 2). The endmember spectra were further applied in the SAM classification method and the diversity indices were calculated based on the classified species and abundance results.

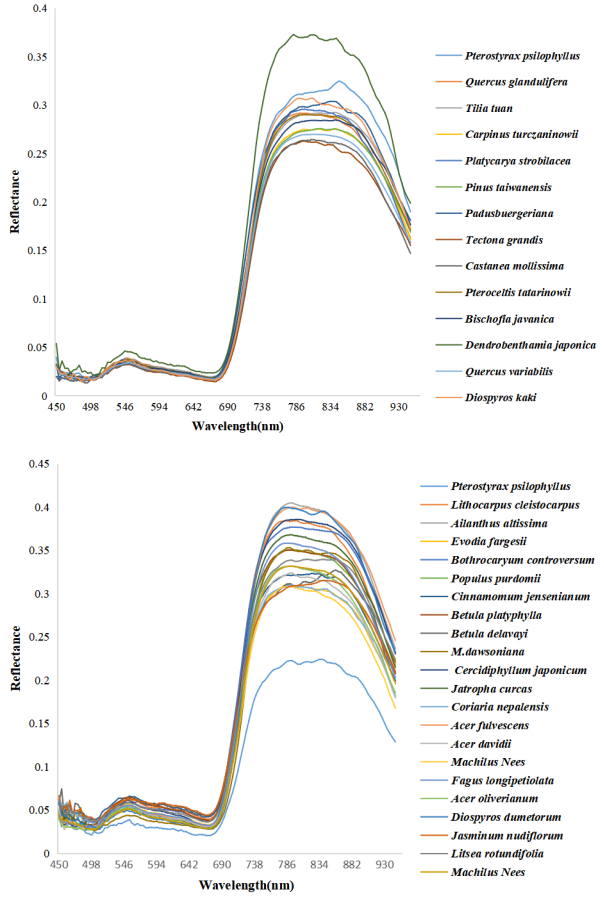


**Figure 2**. Individual tree mean spectra of dominant tree species in two study sites (up: MZL, bottom: GGS)

Aiming at the clustering algorithm developed in remote sensing monitoring of forest species diversity, we firstly explored the association of leaf biochemical diversity, leaf spectral diversity and species diversity, and used the partial least squares regression (PLSR) method to determine the optimal leaf biochemical components that can be well estimated by the leaf spectra. Then we calculated the common-used vegetation indices (VIs) that represent the corresponding biochemical components based on the literature (Table 1). We calculated the standard deviation of VIs for all detected ITCs at each plot, and performed Spearman correlation analysis with the field-measured species diversity indices (corrplot, R-package) to select the optimal VIs. These canopy-level biochemical VIs were then converted into leaf-scale biochemical VIs by dividing them by the ITC's LAI to eliminate the canopy structure effects (Zarco-Tejada et al., 2001; Zhao et al., 2018). In addition, individual-tree structural features were extracted from the terrain-normalized point clouds within the polygons of individual tree crowns (ITCs) segmented by the watershed algorithm (Zhao et al., 2014), and the optimal structural features were selected based on the correlation between the standard deviation of ITC structural features and three species diversity indices.

| Biochemical component | Vegetation index | Reference |
|---|---|---|
| Chl | TCARI/OSAVI | Daughtry et al. (2000); Wu et al. (2008) |
| | VOG1 | Vogelmann et al. (1993) |
| EWT | WBI | Penuelas et al. (1993) |
| Car | CRI | Gitelson et al. (2002) |
| Cel | PRI | Gamon et al. (1992) |
| N | CCCI | El-Shikha et al. (2007) |
| P | NDSI | Patil et al. (2007) |
| SLA | RVI | Jordan (1969) |
| C | PSRI | Merzlyak et al. (1999) |

**Table 1**. Vegetation indices that represent the corresponding biochemical components.

The three clustering algorithms, namely, the self-adaptive Fuzzy C-Means (FCM) algorithm (Zhao et al., 2018), the mean shift algorithm (Cheng, 1995) and the Density-Based Spatial Clustering of Applications with Noise (DBSCAN) algorithm (Ester et al., 1996), were compared in the two representative subtropical forest study areas (i.e., MZL and GGS) based on the optimal leaf biochemical components and structural features to select the optimal clustering algorithm for species diversity estimation. Finally, the estimation results of the optimal clustering algorithm were compared with the spectral angle mapper (SAM) classification method and monitoring methods based on spectral diversity metric (convex hull volume, CHV) and structural heterogeneity index (standard deviation of optimal structural features). The performance and applicability of different remote sensing monitoring methods for forest species diversity indices (species richness, Shannon-Wiener and Simpson index) were explored.

## 3. RESULTS AND DISCUSSIONS

The regression relationships between leaf spectra and biochemical components were established using the PLSR method to determine whether leaf spectra have ability to retrieve leaf biochemical components. In MZL, Chl-a, Chl-b, EWT, Car, SLA, C, Cel, N, Lig and P could be strongly predicted by leaf spectra ($R^2$=0.44–0.82, p<0.01; Table 2) and 7 biochemical VIs (WBI, TCARI/OSAVI, PRI, RVI, CCCI, VOG1, and PSRI) were finally determined. In GGS, Chl-a, Chl-b, EWT, SLA, Cel, N and C could be well estimated by spectral signatures ($R^2$=0.30–0.73, p<0.01) and 3 biochemical VIs (TCARI/OSAVI, RVI, and PSRI) were finally selected.

| Biochemical component | Chl-a | Chl-b | EWT | Car | Cel | N | Lig | P | SLA | C |
|---|---|---|---|---|---|---|---|---|---|---|
| $R^2$ of MZL | 0.80 | 0.81 | 0.78 | 0.82 | 0.44 | 0.74 | 0.67 | 0.61 | 0.80 | 0.81 |
| $R^2$ of GGS | 0.68 | 0.69 | 0.62 | 0.46 | 0.24 | 0.34 | 0.25 | 0.24 | 0.73 | 0.30 |
| RMSE of MZL | 1.87 | 0.96 | 2.76 | 0.30 | 5.99 | 0.35 | 3.43 | 0.02 | 31.35 | 1.25 |
| RMSE of GGS | 2.60 | 1.24 | 4.37 | 0.40 | 3.71 | 0.40 | 3.54 | 0.03 | 34.88 | 1.72 |

**Table 2**. Estimation results of leaf biochemical components.

The ITC segmentation results of all 26 sample plots show that the amounts of segmented ITCs are quantitatively close to the

ground-measured tree number (MZL: $R^2$=0.76, RMSE=5.41; GGS: $R^2$=0.82, RMSE=7.17). Combining the correlation analysis between structural features and field-measured species diversity indices, the two most relevant features, namely canopy cover (CC) and density metric 30% (DM 30%) were selected as the optimal structural features in MZL. And we finally determined five optimal structural features in GGS, including the interquartile range of accumulated elevation (Elev AIQ), coefficient of variance of elevation (Elev CV), the variance of elevation (Elev Var), density metric 20% (DM 20%) and density metric 30% (DM 30%).

Three clustering algorithms were used to estimate species richness, Shannon-Wiener index and Simpson index in the two study areas of MZL and GGS, respectively. Among them, the self-adaptive FCM clustering algorithm had the highest accuracy for estimating species richness, followed by the mean shift algorithm, and the lowest accuracy was obtained by the DBSCAN algorithm (MZL: 0.46>0.16>0.14, GGS: 0.46>0.29>0.23). For the Shannon-Wiener index and Simpson index, the self-adaptive FCM algorithm still obtained the highest accuracy, followed by the DBSCAN algorithm and the mean shift algorithm (Shannon-Wiener index: 0.58>0.26>0.14 for MZL, 0.47>0.36>0.35 for GGS; Simpson index: 0.83>0.28>0.11 for MZL, 0.62>0.19>0.08 for GGS). Therefore, the performance of the self-adaptive FCM clustering algorithm was most stable (Figure 3).

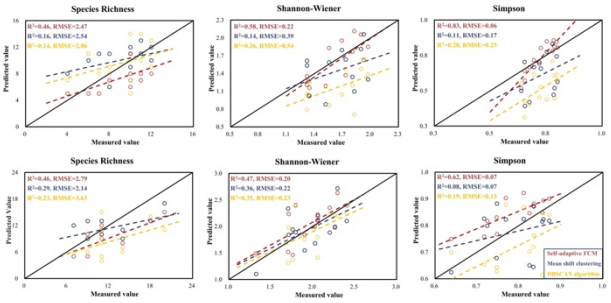


**Figure 3**. Field-measured species diversity indices compared with the predicted values based on three clustering algorithms, namely, the self-adaptive Fuzzy C-Means (FCM) algorithm, the mean shift algorithm and the Density-Based Spatial Clustering of Applications with Noise (DBSCAN) algorithm for MZL (top) and GGS (bottom).

The optimal clustering algorithm (the self-adaptive FCM) was compared with other species diversity monitoring methods. The results showed that the spectral angle mapper (SAM) classification method had the highest accuracy in estimating species richness, followed by the self-adaptive FCM clustering algorithm, and the lowest accuracy was achieved by the spectral diversity metric and the structural heterogeneity index (MZL: 0.62>0.46>0.20>0.20, GGS: 0.55>0.46>0.43>0.07). For the prediction of the Shannon-Wiener index, the SAM classification method performed the best in MZL, followed by the self-adaptive FCM algorithm and the spectral diversity metric, with the lowest prediction accuracy of the structural heterogeneity index (0.64>0.58>0.39>0.02). As for GGS, the SAM classification method also had the highest prediction accuracy, followed by the structural heterogeneity index and the self-adaptive FCM algorithm, with the worst performance of the spectral diversity metric index (0.52>0.48>0.47>0.01). The SAM classification could effectively distinguish the non-dominant species based on hyperspectral data when the endmember spectral library of dominant tree species is available (Zhao et al., 2020). However, when the spectra of non-dominant trees and dominant trees are very similar (such as *Carpinus turczaninowii* and *Castanea mollissima* in this study, Figure 2), SAM classification may also incorrectly classify them, which brings some challenges to the accurate estimation of diversity indices.

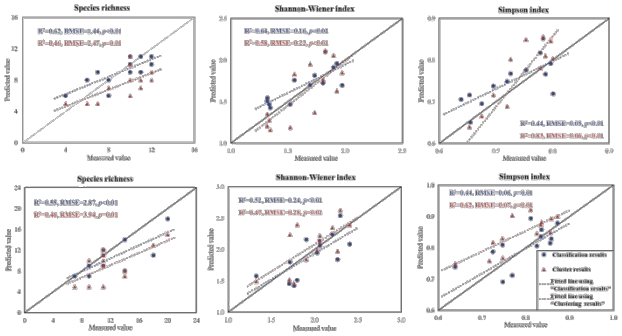


**Figure 4**. Field-measured species diversity indices compared with the predicted values based on classification and clustering approaches for MZL (top) and GGS (bottom).

The results of both study areas showed that the self-adaptive FCM clustering algorithm had the highest prediction accuracy for the Simpson index, followed by the SAM classification method, spectral diversity metric and the structural heterogeneity index (MZL: 0.83>0.44>0.31>0.12, GGS: 0.62>0.44>0.38>0.00; Figure 4, Table 3). This is probably caused by the fact that the Simpson index weights rare species less and dominant species more than Shannon-Wiener index, so the clustering algorithm taking dominant species/traits more into account is expected to predict the Simpson index more accurately. The clustering approach also had the advantage of rapidly capturing forest diversity patterns based on individual tree-based variations in biochemical and structural features without distinguishing the tree species.

| Site | Species diversity | Self-adaptive FCM | SAM | Spectral diversity metric - CHV | Structural heterogeneity index |
|---|---|---|---|---|---|
| MZL | Species Richness | 0.46 | 0.62 | 0.20 | 0.00 |
| | Shannon-Wiener | 0.58 | 0.64 | 0.39 | 0.02 |
| | Simpson | **0.83** | 0.44 | 0.31 | 0.12 |
| GGS | Species Richness | 0.46 | 0.55 | 0.07 | 0.43 |
| | Shannon-Wiener | 0.47 | 0.52 | 0.01 | 0.48 |
| | Simpson | **0.62** | 0.44 | 0.00 | 0.38 |

**Table 3**. Comparison of the accuracy of four monitoring methods.

We applied the optimal diversity estimation approaches to the two study areas covered by the UAV campaigns and mapped forest species diversity indices using a moving window approach with the window size of 30 m × 30 m. Maps of the Simpson index in MZL and GGS estimated by the self-adaptive FCM algorithm are shown in Figure 5.

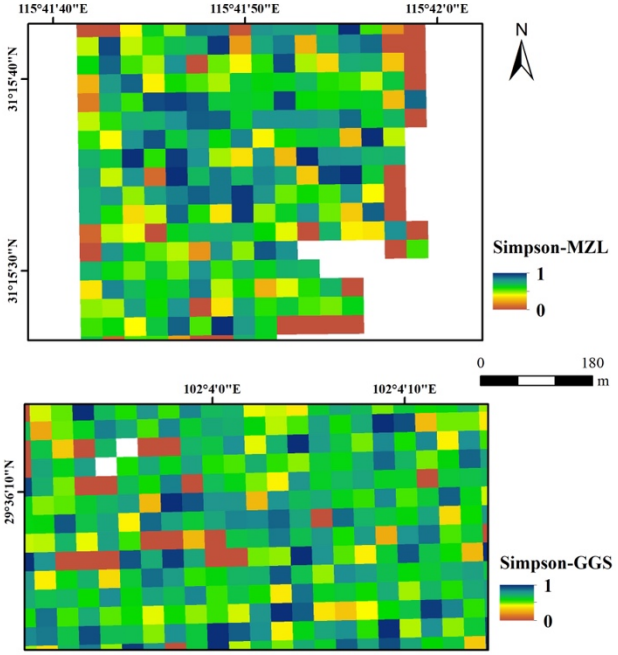


**Figure 5**. Predicted forest canopy species diversity of Simpson index with spatial resolution of 30 m in MZL (top) and GGS (bottom).

## 4. CONCLUSIONS

In this study, we compared the performance of individual tree-based classification, clustering, spectral diversity metric and structural heterogeneity methods with UAV-borne data for estimating the forest species diversity indices in the Mazongling and Gonggashan National Nature Forest Reserves of China. We proved that the SAM classification could provide more accurate predictions of species richness indices but requires spectral information of all dominant tree species. The self-adaptive FCM clustering algorithm could achieve high-precision predictions for evenness indices (especially Simpson index), although information on specific tree species is unavailable. It also revealed that the self-adaptive FCM clustering algorithm had the highest prediction accuracy among other clustering algorithms. The combination of UAV imaging spectroscopy and LiDAR data make it possible to predict regional forest species diversity more accurately at individual canopy scale for complex forests, comparing only using spectral or structural information. Future studies could improve the forest species-spectral library and explore forest species identification from multiple perspectives. For example, considering the variation in forest species characteristics over time, it would be valuable to further examine the accuracy of classification and clustering methods by incorporating phenological or multi-temporal features.

## ACKNOWLEDGEMENTS

This work was supported by the National Natural Science Foundation of China (No. 42071344) and the National Key Research and Development Program of China (2022YFF1302100 and 2020YFE0200800). We thank Ruiying Chang and Qiangxin Ou from the Gonggashan and Mazonglin National Nature Forest Reserves for their support with the fieldwork. We also thank Mingxing Zhang and Shaobo Yang for their assistance in the field measurements.

## REFERENCES

Zheng, Z., Schmid, B., Zeng, Y., Schuman, M.C., Zhao, D., Schaepman, M.E., Morsdorf, F., 2023. Remotely sensed functional diversity and association with productivity in a subtropical forest. *Remote Sens. Environ.*, 290, 113530.

Zheng, Z., Zeng, Y., Schuman, M.C., Jiang, H., Schmid, B., Schaepman, M.E., Morsdorf, F., 2022. Individual tree-based vs pixel-based approaches to mapping forest functional traits and diversity by remote sensing. *Int. J. Appl. Earth Obs. Geoinf.*, 114, 103074.

Zheng, Z., Zeng, Y., Schneider, F.D., Zhao, Y., Zhao, D., Schmid, B., Schaepman, M.E., Morsdorf, F., 2021. Mapping functional diversity using individual tree-based morphological and physiological traits in a subtropical forest. *Remote Sens. Environ.*, 252, 112170.

Li, X., Zheng, Z., Xu, C., Zhao, P., Chen, J., Wu, J., Zhao, X., Mu, X., Zhao, D., Zeng, Y., 2023. Individual tree-based forest species diversity estimation by classification and clustering methods using UAV data. *Front. Ecol. Evol.*, 11, 1139458.

Zhao, Y., Zeng, Y., Zheng, Z., Dong, W., Zhao, D., Wu, B., Zhao, Q., 2018. Forest species diversity mapping using airborne LiDAR and hyperspectral data in a subtropical forest in China. *Remote Sens. Environ.*, 213, 104–114.

Zhao, Y., Zeng, Y., Zhao, D., Wu, B., Zhao, Q., 2016. The optimal leaf biochemical selection for mapping species diversity based on imaging spectroscopy. *Remote Sens.*, 8(3), 216.

Xu, C., Zeng, Y., Zheng, Z., Zhao, D., Liu, W., Ma, Z., Wu, B., 2022. Assessing the impact of soil on species diversity estimation based on UAV imaging spectroscopy in a natural Alpine steppe. *Remote Sens.*, 14 (3), 671.

Wang, R., Gamon J.A., 2019. Remote sensing of terrestrial plant biodiversity. *Remote Sens. Environ.*, 231, 111218.

Zarco-Tejada, P.J., Miller, J.R., Noland, T.L., Mohammed, G.H., Sampson, P.H., 2001. Scaling-up and model inversion methods with narrowband optical indices for chlorophyll content estimation in closed forest canopies with hyperspectral data. *IEEE Trans. Geosci. Remote Sens.*, 39, 1491–1507.

Zhao, D., Pang, Y., Li, Z., Liu, L., 2014. Isolating individual trees in a closed coniferous forest using small footprint lidar data. *Int. J. Remote Sens.*, 35, 7199–7218.

Zhao, D., Pang, Y., Liu, L., Li, Z., 2020. Individual Tree Classification Using Airborne LiDAR and Hyperspectral Data in a Natural Mixed Forest of Northeast China. *Forests*, 11(3), 303.

Cheng, Y., 1995. Mean shift, mode seeking, and clustering. *IEEE Trans. Pattern Anal. Mach. Intell.*, 17, 790–799.

Ester, M., Kriegel, H.P., Sander, J., Xu, X., 1996. A density-based algorithm for discovering clusters in large spatial databases with noise. In: *Second International Conference on Knowledge Discovery and Data Mining: Proceedings*, Amer Assn for Artificial, pp 226–231.

Daughtry, C.S.T., Walthall, C.L., Kim, M.S., De Colstoun, E.B., Mcmurtrey, J.E., 2000. Estimating corn leaf chlorophyll

concentration from leaf and canopy reflectance. *Remote Sens. Environ.*, 74, 229–239.

Wu, C., Niu, Z., Tang, Q., Huang, W.J., 2008. Estimating chlorophyll content from hyperspectral vegetation indices: Modeling and validation. *Agric. For. Meteorol.*, 148, 1230–1241.

Vogelmann, J.E., Rock, B.N., Moss, D.M., 1993. Red edge spectral measurements from sugar maple leaves. *Int. J. Remote Sens.*, 14, 1563–1575.

Penuelas, J., Filella, I., Biel, C., Serrano, L., Save, R., 1993. The reflectance at the 950–970 nm region as an indicator of plant water status. *Int. J. Remote Sens.*, 14, 1887–1905.

Gitelson, A.A., Zur, Y., Chivkunova, O.B., Merzlyak, M.N., 2002. Assessing carotenoid content in plant leaves with reflectance spectroscopy. *Photochem. Photobiol.*, 75, 272–281.

Gamon, J.A., Penuelas, J., Field, C.B., 1992. A narrow-waveband spectral index that tracks diurnal changes in photosynthetic efficiency. *Remote Sens. Environ.*, 41, 35–44.

El-Shikha, D.M., Waller, P., Hunsaker, D., Clarke, T., Barnes, E., 2007. Ground-based remote sensing for assessing water and nitrogen status of broccoli. *Agric. Water Manag.*, 92, 183–193.

Patil, V.D., Adsul, P.B., Deshmukh, L.S., 2007. Studies on spectral reflectance under normal and nitrogen, phosphorus and pest and disease stress condition in soybean (Glycine max L.). *Indian Soc. Remote Sens.,* 35, 351–359.

Jordan, C.F., 1969. Derivation of leaf area index from quality of light on the forest floor. *Ecology*, 50, 663–666.

Merzlyak, M.N., Gitelson, A.A., Chivkunova, O.B., Rakitin, V.Y., 1999. Non-destructive optical detection of pigment changes during leaf senescence and fruit ripening. *Physiol. Plant.*, 106, 135–141.